Bioorganic & Medicinal Chemistry 20 (2012) 4978–4984

Contents lists available at SciVerse ScienceDirect

Bioorganic & Medicinal Chemistry

journal homepage: www.elsevier.com/locate/bmc

Synthesis and biological activity of novel bifunctional isoxazolidinyl polycyclic aromatic hydrocarbons

Antonio Rescifina [a,*], Chiara Zagni [a], Giovanni Romeo [b], Salvatore Sortino [a,*]

[a] Dipartimento di Scienze del Farmaco, Università di Catania, Viale Andrea Doria 6, Catania 95125, Italy
[b] Dipartimento Farmaco-Chimico, Università di Messina, Viale SS. Annunziata, Messina 98168, Italy

ARTICLE INFO

Article history:
Received 13 April 2012
Revised 14 June 2012
Accepted 18 June 2012
Available online 26 June 2012

Keywords:
DNA
Cation recognition
Cycloaddition
Docking
Anticancer agents

ABSTRACT

This paper reports the synthesis and the biological properties of two novel pyrene-bearing isoxazolidinyl derivatives able to exhibit antitumor activity by DNA intercalation. The synthetic approach exploits a consolidated protocol based on 1,3-dipolar cycloaddition reaction. The intercalating properties have been determined by combining electrophoresis studies with molecular docking, while the antitumor activity has been evaluated over five carcinoma cell lines. The obtained compounds show also a good affinity towards silver cations; the presence of a 2-hydroxybenzyl appendage on the isoxazolidine ring ensures a good affinity and selectivity in the binding.

1. Introduction

The discovery of new compounds with antitumor activity has become one of the most important goals in medicinal chemistry. An interesting group of chemotherapeutic agents used in cancer therapy comprises molecules that interact with DNA. The research in this area has revealed a range of DNA recognizing molecules that act as antitumor agents, including groove binders, alkylating agents and intercalator compounds.[1]

Intercalators are molecules that insert perpendicularly into DNA base pairs, exploiting noncovalent bonds.[2] The only recognized forces that maintain the stability of the DNA–intercalators complex, even more stable of than DNA alone, include van der Waals, hydrogen bonding, hydrophobic, and/or charge transfer interactions.[3–6] A DNA intercalator, generally, shows cytotoxic activity when it poisons the Topo enzymes by stabilizing the ternary DNA–intercalator–Topo complex in such a way that the enzymatic process cannot continue forwards or backwards.[7–10]

Recently, we have synthesized a series of ionic and non-ionic isoxazolidinyl polycyclic aromatic hydrocarbons (PAHs) that showed moderate DNA intercalative and cytotoxicity properties (Fig. 1).[11–14]

On the basis of our continuous interest in this area and with the aim to create new DNA intercalators, able to easily diffusable targeting remotely implanted tumors,[15] we have designed the

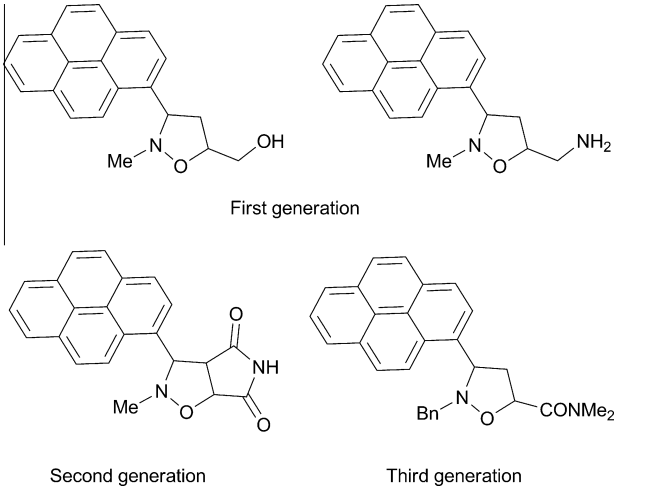

Figure 1. Structures of isoxazolidinyl-PAHs.

novel isoxazolidinyl-PAH template **1** which presents a 2-hydroxybenzyl group at the nitrogen atom (Fig. 2). The reasoning behind our choice is based on the fact that the intercalation is stabilized by hydrogen bond formation. As a consequence, the presence of an appropriately substituted isoxazolidine ring could lead, theoretically, to a better interaction between the hydroxyl groups of PAH and the oxygen atoms of DNA phosphate units.

The intercalating properties of the new compounds have been investigated both in silico, by means of molecular docking, as well

* Corresponding authors. Tel.: +39 095 7385014; fax: +39 06 233208980.
E-mail address: arescifina@unict.it (A. Rescifina).

0968-0896/$ - see front matter © 2012 Elsevier Ltd. All rights reserved.
http://dx.doi.org/10.1016/j.bmc.2012.06.035

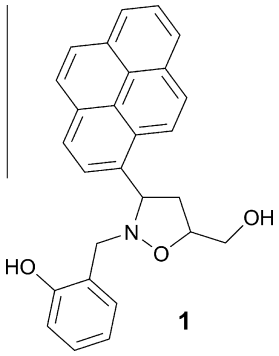

Figure 2. Structure of designed compound **1**.

as in vitro, and the biological activity has been screened over five carcinoma cell lines.

Recently, it has been reported that silver complexes act as antimicrobial agents, interacting with DNA, and that Ag^+ is able to form a metal-mediated base pair complex with the cytosine–cytosine mismatches (C–Ag^+–C) that stabilizes DNA duplex.[16] Moreover, Ag^+ is known to bind with various metabolites, including amine, imidazole, and carboxyl groups, and inactivate sulfhydryl enzymes.[17–19] Many reports in literature deal with on silver bioaccumulation and toxicity;[20–25] thus, the development of sensitive and selective methods for the determination of trace amounts of Ag^+ is of considerable importance.

The structural features of the synthesized compounds suggest a potential affinity towards soft d^{10} transition metal ions such as Ag^+, Tl^+, or Hg^{2+}.[26,27] On the basis of these considerations, we also considerate useful to investigate the potential binding affinity of **1** towards the Ag^+ cation.

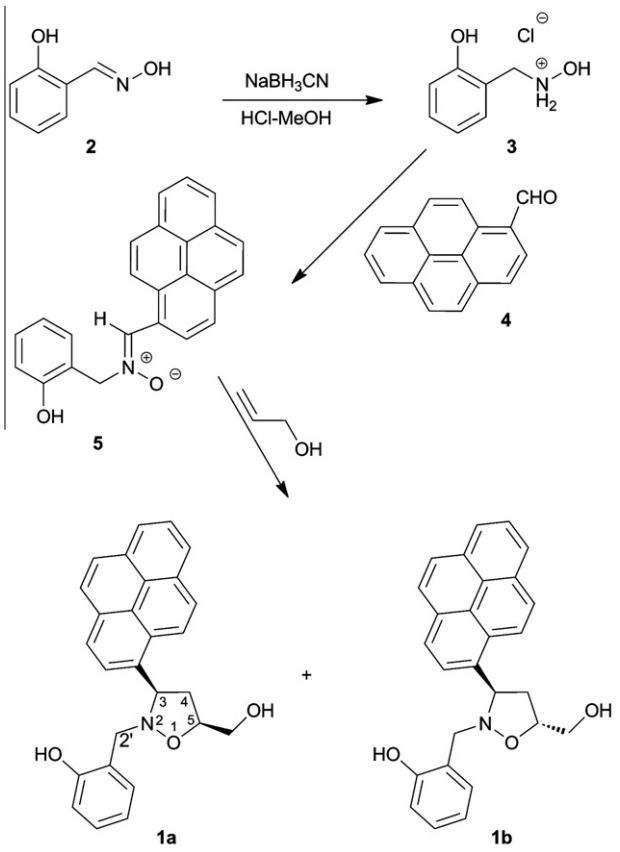

Scheme 1. Synthesis of proposed structure **1**.

2. Results and discussion

2.1. Design

The double function (DNA intercalator and Ag^+ biosensor) can be performed by integrating appropriate functional groups within the same molecular structure. The structural features have to complement the capacity of intercalating well within DNA with a binding site that matches the specific coordination requirements of the target ion and eventually to provide an easily detectable signal upon binding.

The first and third requirements can be obtained by employing a pyrene moiety, that is a well-known intercalating agent and an excellent fluorophore.[2,28,29] Moreover, among the different fluorogenic units, pyrene is particular useful because of its efficient and sensitive monomer emission at 370–430 nm and excimer emission around 480 nm[30,31] with the intensity ratio of excimer to monomer emission being very sensitive to both conformational changes and guest ion concentration.[31–34]

The presence of an appropriately substituted isoxazolidine ring could ensure the second requirement. In fact, compounds containing nitrogen or sulfur atoms, which are soft ligands according to the 'hard and soft acids and bases' theory, possess great affinity toward the soft d^{10} transition-metal ions such as Ag^+, Tl^+ or Hg^{2+}.[26,27] In view of the molecular structure of **1**, we expect the fluorescence of the pyrene fluorophore to be quenched, via photoinduced electron transfer, due to the presence of the close nitrogen atom of the isoxazolidine ring. Binding with metal cation is expected to restore the fluorescence.[35,36]

At the same time, the presence of hydroxyl groups could play an important role in the DNA-recognizing region because of their ability to form favorable intermolecular hydrogen bonds[37–40] with the DNA backbone. This could contribute to the formation of stable complexes, and then to a better interaction with DNA sites. In addition, hydroxyl groups are expected to play a role in the coordination of the metal cations, favoring the formation of the coordination complexes.

On the basis of these considerations we designed compound **1** where the isoxazolidine core was functionalized with 1-pyrenyl, hydroxymethyl and 2-hydroxybenzyl groups in positions 3, 5 and 2, respectively (Fig. 2).

2.2. Synthesis

As shown in Scheme 1, the target compound **1** was synthesized employing the 1,3-dipolar cycloaddition reaction, according to an already consolidated synthetic protocol.[11–14] The functionalized nitrone **5** was prepared in high yield by reaction of salicylhydroxylamine **3**,[14] obtained by the reduction of the commercially available salicylaldoxime **2**, with 1-pyrenylcarboxaldehyde. Successively, the reaction of nitrone **5** with allyl alcohol, performed in dry toluene and in sealed tube at 120 °C for 12 h, using a 1:1.5 relative ratio of dipole to dipolarophile, afforded only the 5-regioisomeric PAH-isoxazolidines **1a**,**b** with a (C_3,C_5)-*cis*/(C_3,C_5)-*trans* ratio of 1.3:1 and a total yield of 89%.

The regiochemistry of the cycloaddition process was readily deduced by ^{1}H NMR measurements. For the isoxazolidines at hand, the H_{4a} and H_{4b} protons are well separated from H_5, giving rise to a well resolved ABX pattern, whilst in 4-substituted isoxazolidines the same protons resonate at reasonably similar fields and often merge in complex unresolved signals.[41–44]

The relative *cis*/*trans* configuration of the isoxazolidine ring substituents was assigned on the basis of NOE experiments (see supplementary material).

Table 1
Evaluation of cytotoxicity for compounds **1** by MTS or SRB assay[a]

Compound	IC_{50}[b] (μM)					
	HeLa	A-549	Molt-3	THP-1	U-937	Vero
1a	4	2	5	7	32	37
1b	11	9	13	15	88	103
Actinomycin D	—	—[c]	<1[d]	—	<1[d]	11[d]

[a] Cells were exposed in optimal culture conditions in 96-well plates to five concentrations of the compounds (1, 10, 100, 200, 500 μM) or control medium for 20 h before determining cellular metabolic activity by a MTS tetrazolium compound bioreduction assay or sulforhodamine B assay.
[b] Each value was determined from triplicate samples using a non-linear regression analysis.
[c] Literature data[46] reported that at a concentration of 0.5 μg/mL of actinomycin D the number of A-549 cells declined to 40% of the control at 8 h.
[d] Data from literature.[11]

2.3. Biological evaluation

Taking into account the pharmacological potential of this class of compounds, the cytotoxicity against a panel of tumor or normal cell lines was evaluated.

The cytotoxicity was assessed in vitro against human cervical carcinoma (HeLa), human lung cancer (A-549), a panel of leukemia (Molt-3, THP-1) and lymphoma (U-937), as well as against normal African green monkey kidney (Vero) cell lines. As a screening assay, the cytotoxicity was tested using a MTS tetrazolium reduction assay, except for A-549 cell lines, and expressed as IC_{50} values. For A-549 cell lines, the growth inhibition was tested by the sulforhodamine B (SRB) assay[45] where IC_{50} is the drug concentration (μM) that yields 50% less cells than the drug-free control. The results shown in Table 1 indicate that Vero cells were more resistant than tumoral cell lines to the toxicity induced by new synthesized compounds, whereas both compounds showed a high level of cytotoxicity against A-549 cell lines. In particular, the new derivative **1a** showed an improved cytotoxic activity, with respect to compounds previously reported by us,[11–14] that are almost comparable with that of actinomycin D, a well-known intercalating agent.

Analogously to the precedent isoxazolidine series[11–14] (Fig. 1), the *cis*/*trans* configuration has a weak influence on the cytotoxicity, but in this case the *cis* isomer is more active of the *trans* one. In any case, compound **1a** shows activity on all the tested cell lines and the cytotoxicity against A-549 cells with an IC_{50} of 2 μM is interesting.

2.4. DNA binding properties and molecular docking

Compound **1a**, which shows the highest cytotoxicity, has been used as a model to investigate the DNA intercalation. Thus, incubation of **1a** with ΦX174 RF I, a double-stranded circular DNA molecule, followed by electrophoretic examination, showed characteristic streaking of the supercoiled species, indicative of intercalation (see Supplementary Materials).[47]

In order to confirm and rationalize these biological results as well as to gain more insight into the intercalation modality, the supramolecular complexes of synthesized compounds with DNA have been investigated by molecular modeling methodology. Although the obtained compounds are racemates, we have already demonstrated that compounds with a 3*R* configuration possess the best intercalating properties.[13] Thus, all molecular docking calculations were performed on 3*R* stereoisomers, making use of an already consolidate procedure.[13,14]

The possibility to achieve complexes by binding along the groove was a priori excluded according to previously reported results.[12]

The obtained results, reported in Table 2, showed that isoxazolidinyl-PAH **1a** has the best intercalative properties, exhibiting the highest activity, according to the biological results. Moreover, **1a** shows a clear preference for the poly-GC fragment intercalating from the minor groove. The insertion of a 2-hydroxybenzyl functionality on the isoxazolidine nitrogen atom, leads to a better interaction with the base pairs with respect to the intercalation observed with the protonated aminomethyl derivative (Fig. 1).

The results of docking calculations (Fig. 3) show compound (3*R*,5*S*)-**1a** intercalated into poly-d$(G–C)_2$ from minor groove; this ligand engages three hydrogen bonds, one between the hydroxymethyl oxygen atom and the aminic hydrogen of G8 nucleobase and the other two between the phenolic and hydroxymethylic hydrogens with the backbone rybosyl oxygens of G8 and C9 nucleobases, respectively. Moreover, it is evident the extensive stabilization due to the hydrophobic and van der Waals interactions, evidenced by wireframe spheres that represent the atoms in close contact.

Table 2
Calculated binding energies for compounds **1** intercalated in d$(A–T)_2$ and d$(G–C)_2$ dodecamers

Compound	Poly-AT	
	From major groove	From minor groove
(3*R*,5*S*)-**1a** (*cis*)	−10.04[a]	−11.38
(3*R*,5*R*)-**1b** (*trans*)	−9.97	−11.12
	Poly-GC	
	From major groove	From minor groove
(3*R*,5*S*)-**1a** (*cis*)	−9.99	−12.47
(3*R*,5*R*)-**1b** (*trans*)	−9.38	−11.79

[a] All values are in kcal/mol.

2.5. Cation recognition properties

Figure 4 shows the fluorescence emission spectra of compound **1a** in water:ethanol (1:1) (spectrum a). Although the spectral shape was identical to what typical expected for a pyrene fluorogenic center,[30,31] the emission quantum yield was more than one order of magnitude smaller than that of 1-pyrene methanol, chosen as a model reference compound (spectrum b). This suggests a remarkable interaction between the excited singlet state of pyrene and the isoxazolidinyl appendage. As far as the fluorescence quenching mechanism is concerned, a photoinduced energy transfer is of course out of question because it is highly exoergonic. The excited singlet state of pyrene is in fact several kcal/mol below than those of both the isoxazolidinyl and the phenol appendages. On the other hand, the quenching observed is more likely due to a photoinduced electron transfer between the nitrogen atom of the isoxazolidinyl substituent and the excited singlet state of the pyrene chromophore. This hypothesis is supported by fluorescence experiments carried out at different p*H* values which showed a significant revival of the pyrene fluorescence with the decrease of p*H*. In fact, by monitoring the fluorescence intensity at 395 nm as a function of p*H* (inset Fig. 4), a sigmoidal trend with an inflection

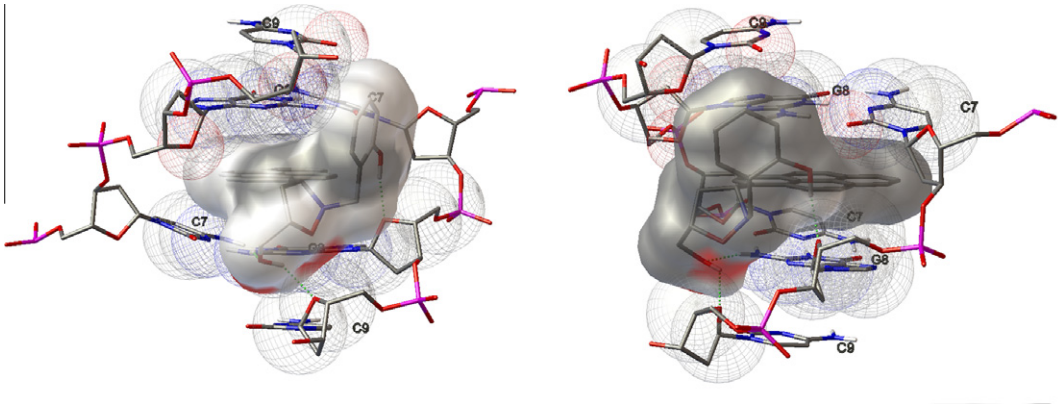

Figure 3. Illustration of compound **1a** intercalated into poly-d(G–C)$_2$ from minor groove. Front view (left) and side view (right). Spheres displayed as wireframe represent atoms in close contact.

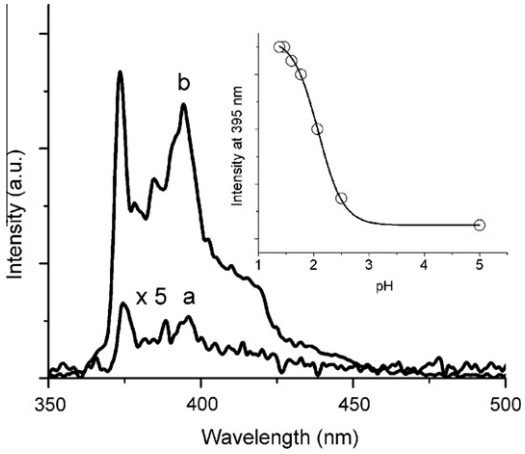

Figure 4. Fluorescence emission spectra of **1a** (a) and an optically matched solution of 1-pyrene methanol (b) in water:ethanol (1:1). λ_{exc} = 345 nm; T = 25 °C. Spectrum (a) has been multiplied by a factor 5 for sake of clarity. The inset shows the fluorescence intensity of **1a** as a function of pH.

point around p*H* ca. 2.1 was obtained, according to the typical pK_a values reported for the isoxazolidine-derivatives.[48] Therefore, according to our logical design, **1a** is in a 'fluorescence-OFF' state under neutral p*H* conditions.

This represents an ideal requisite to investigate the affinity of **1a** towards Ag^+ cations by fluorescence spectroscopy. In fact, on the basis of the above results, coordination of the nitrogen binding site with the metal ion should, in principle, switch the fluorescence of **1a** in an 'ON' state. To this end, we performed fluorescence measurements by adding increasing concentrations of Ag^+ on a solution of **1a** (6 μM). The results illustrated in Figure 5a, show that the presence of Ag^+ leads to a significant increase of the fluorescence intensity which reaches a saturation value at a concentration of ca. 400 μM. Addition of other metal cations such as Na^+, K^+, Ni^{2+}, Co^{2+}, Zn^{2+}, Cd^{2+}, and Hg^{2+} to different fresh solutions of **1a** under identical experimental conditions had a less pronounced effect on the fluorescence of **1a** which slightly increased but did not reach any saturation in the range of the concentrations explored.

Figure 5b shows the intensity increase monitored at 395 nm as a function of the concentration of the metal cations from which appears evident a good selectivity of **1a** for Ag^+. The linearity of the Benesi-Hildebrand titration plot of **1** with Ag^+ (data not shown) shows a **1a**:Ag^+ ratio of 1:1 and a binding constant of ca. 4×10^2 M^{-1}.

Analogous experiments conducted on compound **1b** showed no significant increase of the fluorescence intensity indicating that

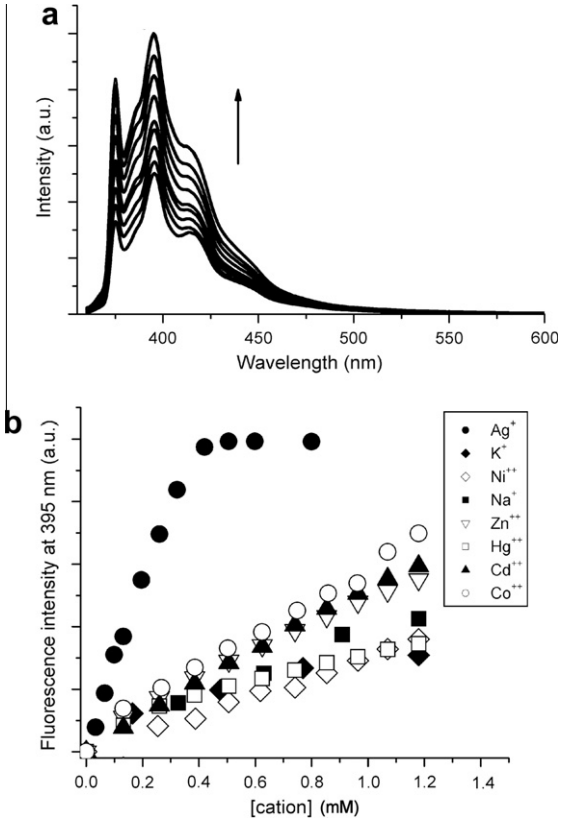

Figure 5. (a) Fluorescence emission spectra of **1a** in the presence of increasing amounts of Ag^+ in the range 0–0.8 mM (bottom to top). (b) Fluorescence intensity of **1a** in the presence of increasing amounts of metal cations. Water:ethanol (1:1), λ_{exc} = 345 nm; T = 25 °C.

there is not a perceptible formation of a complex. This is in accord with the quantomechanical calculated energies, at DFT level of theory, of the full optimized complexes obtained for interaction of compounds **1a** and **1b** with silver cation. The silver complex achieved with compound **1a** was 4.4 kcal/mol more stable respect to the one with **1b**, according to a binding model involving the coordination of Ag^+ with the nitrogen of the isoxazolidinyl and the oxygens of the phenolic and hydroxymethylic appendages. On the contrary, in the case of compound **1b**, the *trans* rearrangement of the hydroxymethylic substituent precludes the tetracoordination weakening the complex formation (Fig. 6).

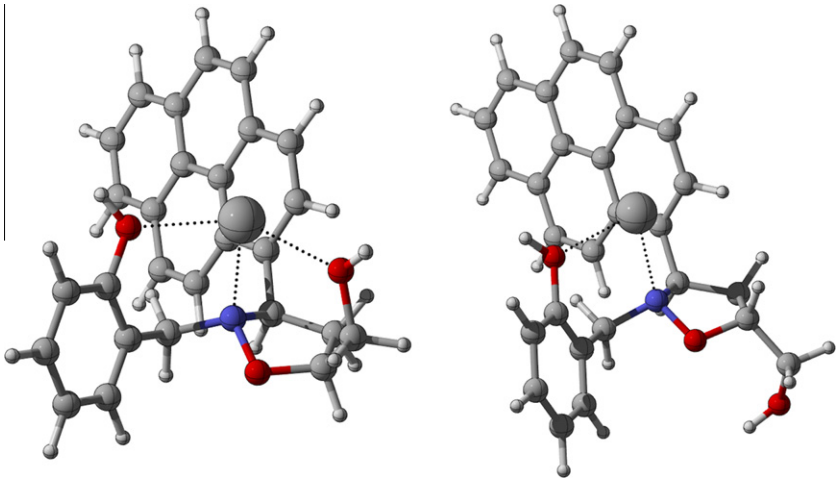

Figure 6. Complex of **1a** (left) and **1b** (right) with Ag^+ optimized at DFT level of calculation.

3. Conclusions

The synthesis and biological properties of two novel bifunctional pyrene-bearing isoxazolidinyl derivatives have been reported. The obtained compounds show an interesting antitumor activity, due to DNA intercalation, over five carcinoma cell lines. The intercalating properties, determined by electrophoresis are consistent with molecular docking studies.

Compound **1a** shows also a relevant selectivity towards Ag^+ cation. Noteworthy, as Ag^+ belongs to transition-metal ions, which usually quench fluorescence emission, this result appears interesting because only a few fluorescent sensors for detecting silver ion have been reported to date.

These derivatives could be of use in the search of compounds characterized by antitumor activity, according to continuous efforts in the synthesis of new DNA-intercalating agents. Moreover, their concomitant capacity to selectively complex with silver cations opens new ways to bifunctional biologically active compounds.

4. Experimental

4.1. General methods

Solvents and reagents were used as received from commercial sources. Melting points were determined with a Kofler apparatus and are reported uncorrected. Elemental analyses were performed with a Perkin–Elmer elemental analyzer. NMR spectra (^{1}H NMR recorded at 500 MHz, ^{13}C NMR recorded at 125 MHz) were obtained on Varian Instruments and are referenced in ppm relative to TMS or the solvent signal. Thin-layer chromatographic separations were performed on Merck silica gel 60-F_{254} precoated aluminum plates. Flash chromatography was accomplished on Merck silica gel (200–400 mesh).

4.2. Synthesis

4.2.1. Synthesis of salicylhydroxylamine hydrochloride 3

To a solution of the salicylaldoxime **2** (3.0 g, 21.9 mmol) in dry methanol (24 mL), containing a trace of methyl orange, $NaBH_3CN$ (1.37 g, 21.9 mmol) was added. Subsequently, 2.5 M HCl–MeOH was added dropwise with stirring to maintain the red color of the solution for 30 min. The reaction mixture was further stirred for 4 h, and methanol was removed in vacuo to give a white solid. Yield 96%; m.p. 71–75 °C. ^{1}H NMR (500 MHz, $CDCl_3$:CD_3OD 1:1, 27 °C, TMS): δ = 4.39 (s, 2H, CH_2), 6.86–7.33 (m, 4H). ^{13}C NMR (125 MHz, $CDCl_3$:CD_3OD 1:1, 27 °C, CD_3OD): δ = 52.68, 116.27, 116.34, 120.88, 132.61, 133.27, 157.74. Anal. Calcd for $C_7H_9NO_2$·HCl: C, 47.88; H, 5.74; N, 7.98. Found: C, 47.73; H, 5.75; N, 7.96.

4.2.2. Synthesis of *C*-(1-pyrenyl)-*N*-(2-idroxybenzyl)nitrone 5

To a solution of sodium acetate (0.29 g, 3.0 mmol) in dichloromethane (30 mL), cooled at 0 °C, was added the salicylhydroxylamine hydrochloride **2** (500 mg, 3.6 mmol) and successively, dropwise, the corresponding 1-pyrenylcarboxaldehyde **4** (0.69 g, 3,0 mmol). The reaction mixture was then stirred for 1 h at 0 °C and then at room temperature overnight. After this time, organic solvent was removed under reduced pressure and the obtained solid was purified by silica gel flash-chromatography (MeOH/$CHCl_3$ 5:95) to give the pure nitrone **5** that was re-crystallized from ethyl acetate/cycloexane. *Z*/*E* ratio = 88:1. Yield 92%; yellow solid, mp 198–202 °C. *Z*-isomer ^{1}H NMR (500 MHz, $CDCl_3$:CD_3OD 1:1, 27 °C, TMS): δ = 5.33 (s, 2H, CH_2), 6.90–8.18 (m, 12H), 8.52 (s, 1H, HC≡N), 9.51 (d, J = 7.8 Hz, 1H, H_9). ^{13}C NMR (125 MHz, $CDCl_3$:CD_3OD 1:1, 27 °C, CD_3OD): δ = 67.84, 116.99, 120.77, 121.09, 122.40, 125.23, 125.37, 126.90, 127.19, 128.00, 128.10, 129.04, 129.93, 130.65, 131.69, 132.14, 132.55, 158.40. Anal. Calcd for $C_{24}H_{17}NO_2$: C, 82.03; H, 4.88; N, 3.99. Found: C, 82.25; H, 4.87; N, 3.99.

4.2.3. Synthesis of isoxazolidinyl-PAHs 1

A solution of nitrone **5** (0.2 g, 0.57 mmol) in toluene (10 mL) and allyl alcohol (7 mL, 0.85 mmol) placed in a sealed tube equipped with a stir bar, was heated at 120 °C for 12 h. The mixture was evaporated and the resulting solid was purified by flash-chromatography on a silica gel with cyclohexane/ethyl acetate (60:40) as eluent.

First eluted product: 2-{[(3*RS*,5*SR*)-5-(hydroxymethyl)-3-pyren-1-ylisoxazolidin-2-yl]methyl}phenol **1a**. Yield 50%, white sticky solid; ^{1}H NMR (500 MHz, $CDCl_3$, 27 °C, TMS): δ = 2.51 (m, 1H, H_{4a}), 3.14 (ddd, 1H, J = 7.0, 8.6 e 13.1 Hz, H_{4b}), 3.79 (d, 2H, CH_2OH), 4.04 (d, 1H, J = 14.3 Hz, $H_{2'a}$), 4.30 (d, 1H, J = 14.3 Hz, $H_{2'b}$), 4.63 (m, 1H, H_5), 5.05 (t, 1H, J = 7.0 Hz, H_3), 6.74–8.32 (m, 13H). ^{13}C NMR (125 MHz, $CDCl_3$, 27 °C, $CDCl_3$): δ = 40.10, 59.01, 64.35, 69.94, 78.31, 116.51, 119.17, 119.64, 120.91, 121.70, 122.30, 123.82, 125.04, 125.26, 125.62, 126.14, 127.36, 127.70, 128.27, 128.84, 129.00, 130.47, 131.75, 157.79. Anal. Calcd for $C_{27}H_{23}NO_3$: C, 79.20; H, 5.66; N, 3.42. Found: C, 79.03; H, 5.65; N, 3.43.

Second eluted product: 2-{[(3*RS*,5*RS*)-5-(hydroxymethyl)-3-pyren-1-ylisoxazolidin-2-yl]methyl}phenol **1b**. Yield 39%, white sticky solid; ^{1}H NMR (500 MHz, $CDCl_3$, 27 °C, TMS): δ = 1.94 (br s, 1H, J = 2.7 Hz, OH), 2.66 (m, 1H, H_{4a}), 3.01 (m, 1H, H_{4b}), 3.71 (d, 1H, J = 14.4 Hz, $H_{5a'}$), 3.95 (d, 1H, J = 14.4 Hz, $H_{5b'}$), 4.03 (d, 1H,

J = 13.3 Hz, $H_{2'a}$), 4.32 (d, 1H, J = 13.3 Hz, $H_{2'b}$), 4.59 (m, 1H, H_5), 4.97 (m, 1H, H_3), 6.73–8.36 (m, 13H), 9.63 (s, 1H, OH). ^{13}C NMR (125 MHz, $CDCl_3$, 27 °C, $CDCl_3$): δ = 39.72, 58.01, 62.83, 66.99, 78.78, 116.54, 119, 62, 121.07, 121.90, 124.37, 124.78, 124.96, 125.09, 125.36, 125.49, 125.67, 126.18, 126.27, 127.39, 127.76, 128.31, 128.43, 128.82, 129.03, 130.57, 131.37, 156.64. Anal. Calcd for $C_{27}H_{23}NO_3$: C, 79.20; H, 5.66; N, 3.42. Found: C, 79.38; H, 5.67; N, 3.41.

4.3. Biological assay methods

4.3.1. Evaluation of cytotoxicity with MTS assay

Cytotoxicity of all compounds was evaluated by a commercial viability assay (CellTiter 96® Aqueous One Solution Assay, Promega Co., Madison WI), according to the Manufacturer's instructions. This assay is based on the principle that cells, at death, rapidly lose the ability to reduce MTS tetrazolium. Briefly, HeLa, MOLT-3, U-937, THP-1 and Vero cells were cultured in optimal culture conditions for 20 h in 96-well plates, in the absence of the compounds or in their presence, at concentrations ranging from 1 μM to 500 μM. At the end of the incubation time, the MTS-tetrazolium-based reagent was added to each well. After a further incubation of one hour at 37 °C in a humidified, 5% CO_2 atmosphere, the absorbance of the samples was recorded at 490 nm using a 96-well spectrophotometer. The assays were performed in triplicate. The inhibitory concentrations 50 (IC_{50}) were calculated as the concentrations of the compounds required to cause 50% reduction of absorbance values. For all compounds a non-linear regression analysis was used.

4.3.2. Evaluation of cytotoxicity with SRB assay

TCA-fixed cells were stained for 30 min with 0.4% (wt/vol) SRB dissolved in 1% acetic acid. At the end of the staining period, SRB was removed and cultures were quickly rinsed four times with 1% acetic acid to remove unbound dye. The acetic acid was poured directly into the culture wells from a beaker. Residual wash solution was removed by sharply flicking plates over a sink, which ensured the complete removal of rinsing solution. After being rinsed, the cultures were air dried until no standing moisture was visible. Bound dye was solubilized with 10 mM unbuffered Tris base (pH 10.5) for 5 min on a gyratory shaker.

OD was read in a UVmax microtiter plate reader (Molecular Devices, Menlo Park, CA). For maximum sensitivity, OD was measured at 564 nm.

4.3.3. ΦX174. RF I DNA unwinding assay

Reaction mixtures (10 μL final volume) contained 0.3 μg supercoiled φX174 RF I DNA in reaction buffer (10 mM Tris·HCl, p*H* 7.5, 50 mM KCl, 5 mM $MgCl_2$, 0.1 mM EDTA, and 15 μg/mL bovine serum albumin) and 2 units of Top1.[47] Reactions were performed at 37 °C for 30 min with Top1 alone followed by incubation in the presence or absence of drug for another 30 min. The reactions were terminated by the addition of 0.5% SDS and 0.5 mg/mL proteinase K. Samples were incubated for 30 min at 50 °C. Next, 1.2 μL of 10× loading buffer (20% Ficol 400; 0.1 M Na_2EDTA, pH 8.0, 1.0% SDS, and 0.25% bromphenol blue) were added and reactions mixtures were loaded onto a 1% agarose gel made in 1× TBE buffer. Gels were run in 1× TBE containing 0.1% SDS. After electrophoresis, DNA bands were stained in ethidium bromide (10 μg/mL) and visualized by transillumination with ultraviolet light (300 nm).

4.4. Molecular docking

All poly-d(A–T)$_2$ and poly-d(G–C)$_2$ fragments were 3′- and 5′-endcapped with a phosphate group and the system configured as a fully anionic oligonucleotide. Subsequently, the geometry was fully minimized with a convergence criterion of 0.005 kcal/molÅ, assigning a distance-dependent dielectric of 1.0, 1–4 scale factors of 0.833 for the electrostatic part and of 0.5 for the van der Waals one, and the nonbonded cutoff on off.

For fine docking with AutoDock 4.2.3 we used the following parameters: grid spacing = 0.375 Å, number of runs = 25, npts = 60 60 60 centered on the pocket, ga_num_evals = 200,00,000, ga_pop_size = 150 and ga_num_generations = 27,000. The graphical user interface AutoDockTools (1.5.6rc1, R45)[49] was used for establishing the Autogrid points as well as visualization of docked ligand-nucleic acid structures.

4.5. Fluorescence experiments

Fluorescence spectra have been carried out with a Fluorolog-2 (mod. F-111) spectrofluorimeter. All the spectra have been corrected for the different fraction of absorbed photons due to the slight dilution of the starting sample after addition of the stock solutions of metal cations.

Supplementary data

Supplementary data associated with this article can be found, in the online version, at http://dx.doi.org/10.1016/j.bmc.2012.06.035.

References and notes

1. Pindur, U.; Jansen, M.; Lemster, T. *Curr. Med. Chem.* **2005**, *12*, 2805.
2. Martinez, R.; Chacon-Garcia, L. *Curr. Med. Chem.* **2005**, *12*, 127.
3. Baginski, M.; Fogolari, F.; Briggs, J. M. *J. Mol. Biol.* **1997**, *274*, 253.
4. Rehn, C.; Pindur, U. *Monatsh. Chem.* **1996**, *127*, 631.
5. Shui, X. Q.; Peek, M. E.; Lipscomb, L. A.; Gao, Q.; Ogata, C.; Roques, B. P.; Garbay-Jaureguiberry, C.; Wilkinson, A. P.; Williams, L. D. *Curr. Med. Chem.* **2000**, *7*, 59.
6. Waring, M. J.; Bailly, C. B. *Gene* **1994**, *149*, 69.
7. Burden, D. A.; Osheroff, N. *Biochim. Biophy. Acta Gene Struct Expr* **1998**, *1400*, 139.
8. Froelichammon, S. J.; Osheroff, N. *J. Biol. Chem.* **1995**, *270*, 21429.
9. Pommier, Y.; Pourquier, P.; Fan, Y.; Strumberg, D. *Biochimica Et Biophysica Acta-Gene Structure and Expression* **1998**, *1400*, 83.
10. Stivers, J. T.; Harris, T. K.; Mildvan, A. S. *Biochemistry (Mosc.)* **1997**, *36*, 5212.
11. Rescifina, A.; Chiacchio, M. A.; Corsaro, A.; De Clercq, E.; Iannazzo, D.; Mastino, A.; Piperno, A.; Romeo, G.; Romeo, R.; Valveri, V. *J. Med. Chem.* **2006**, *49*, 709.
12. Rescifina, A.; Chiacchio, U.; Piperno, A.; Sortino, S. *New J. Chem.* **2006**, *30*, 554.
13. Rescifina, A.; Chiacchio, U.; Corsaro, A.; Piperno, A.; Romeo, R. *Eur. J. Med. Chem.* **2011**, *46*, 129.
14. Rescifina, A.; Varrica, M. G.; Carnovale, C.; Romeo, G.; Chiacchio, U. *Eur. J. Med. Chem.* **2012**, *51*, 163.
15. Denny, W. A.; Atwell, G. J.; Baguley, B. C. *Anti-Cancer Drug Des.* **1987**, *2*, 263.
16. Ono, A.; Cao, S.; Togashi, H.; Tashiro, M.; Fujimoto, T.; Machinami, T.; Oda, S.; Miyake, Y.; Okamoto, I.; Tanaka, Y. *Chem. Commun. (Camb.)* **2008**, 4825.
17. Feng, Q. L.; Wu, J.; Chen, G. Q.; Cui, F. Z.; Kim, T. N.; Kim, J. O. *J. Biomed. Mater. Res.* **2000**, *52*, 662.
18. Lansdown, A. B. *J. Wound Care* **2002**, *11*, 125.
19. Yamanaka, M.; Hara, K.; Kudo, J. *Appl. Environ. Microbiol.* **2005**, *71*, 7589.
20. Ganjali, M. R.; Norouzi, P.; Alizadeh, T.; Adib, M. J. *Braz. Chem. Soc.* **2006**, *17*, 1217.
21. Matsuda, K.; Hiratsuka, N.; Koyama, T.; Kurihara, Y.; Hotta, O.; Itoh, Y.; Shiba, K. *Clin. Chem.* **2001**, *47*, 763.
22. Peng, H. Q.; Brooks, B. W.; Chan, R.; Chyan, O.; La Point, T. W. *Chemosphere* **2002**, *46*, 1141.
23. Ratte, H. T. *Environ. Toxicol. Chem.* **1999**, *18*, 89.
24. Wan, A. T.; Conyers, R. A. J.; Coombs, C. J.; Masterton, J. P. *Clin. Chem.* **1991**, *37*, 1683.
25. Zhang, X. B.; Han, Z. X.; Fang, Z. H.; Shen, G. L.; Yu, R. Q. *Anal. Chim. Acta* **2006**, *562*, 210.
26. Badr, I. H. A. *Microchim. Acta* **2005**, *149*, 87.
27. Yamamoto, C.; Seto, H.; Ohto, K.; Kawakita, H.; Harada, H. *Anal. Sci.* **2011**, *27*, 389.
28. Cho, N.; Asher, S. A. *J. Am. Chem. Soc.* **1993**, *115*, 6349.
29. Jiang, Z. H.; Zhang, Y. H.; Yu, Y.; Wang, Z. Q.; Zhang, X.; Duan, X. R.; Wang, S. *Langmuir* **2010**, *26*, 13773.
30. Fabbrizzi, L.; Poggi, A. *Chem. Soc. Rev.* **1995**, *24*, 197.
31. Winnik, F. M. *Chem. Rev.* **1993**, *93*, 587.
32. de Silva, A. P.; Fox, D. B.; Huxley, A. J. M.; Moody, T. S. *Coord. Chem. Rev.* **2000**, *205*, 41.
33. Lewis, F. D.; Zhang, Y. F.; Letsinger, R. L. *J. Am. Chem. Soc.* **1997**, *119*, 5451.
34. Prodi, L.; Bolletta, F.; Montalti, M.; Zaccheroni, N. *Coord. Chem. Rev.* **2000**, *205*, 59.
35. Draxler, S.; Lippitsch, M. E. *Sensors and Actuators B-Chemical* **1995**, *29*, 199.

36. Inada, T. N.; Kikuchi, K.; Takahashi, Y.; Ikeda, H.; Miyashi, T. *J. Photochem. Photobiol. A* **2000**, *137*, 93.
37. Favier, A.; Blackledge, M.; Simorre, J. P.; Crouzy, S.; Dabouis, V.; Gueiffier, A.; Marion, D.; Debouzy, J. C. *Biochemistry (Mosc.)* **2001**, *40*, 8717.
38. Pohle, W.; Bohl, M.; Flemming, J.; Bohlig, H. *Biophys. Chem.* **1990**, *35*, 213.
39. Usha, S.; Johnson, I. M.; Malathi, R. *J. Biochem. Mol. Biol* **2005**, *38*, 198.
40. Vonszentpaly, L.; Shamovsky, I. L. *Mol. Pharmacol.* **1995**, *47*, 624.
41. Burdisso, M.; Gandolfi, R.; Grunanger, P. *Tetrahedron* **1989**, *45*, 5579.
42. Merino, P.; Revuelta, J.; Tejero, T.; Chiacchio, U.; Rescifina, A.; Piperno, A.; Romeo, G. *Tetrahedron Asymmetry* **2002**, *13*, 167.
43. Chiacchio, U.; Corsaro, A.; Mates, J.; Merino, P.; Piperno, A.; Rescifina, A.; Romeo, G.; Romeo, R.; Tejero, T. *Tetrahedron* **2003**, *59*, 4733.
44. Romeo, G.; Iannazzo, D.; Piperno, A.; Romeo, R.; Corsaro, A.; Rescifina, A.; Chiacchio, U. *Mini-Rev. Org. Chem.* **2005**, *2*, 59.
45. Skehan, P.; Storeng, R.; Scudiero, D.; Monks, A.; Mcmahon, J.; Vistica, D.; Warren, J. T.; Bokesch, H.; Kenney, S.; Boyd, M. R. J. *Natl. Cancer Inst.* **1990**, *82*, 1107.
46. Watanabe, N.; Dickinson, D. A.; Krzywanski, D. M.; Iles, K. E.; Zhang, H. G.; Venglarik, C. J.; Forman, H. J. *Am. J. Physiol. Lung Cell. Mol. Phy.* **2002**, *283*, L726.
47. Pommier, Y.; Covey, J. M.; Kerrigan, D.; Markovits, J.; Pham, R. *Nucleic Acids Res.* **1987**, *15*, 6713.
48. Hjeds, H.; Jerslev, B.; Ross-Petersen, K. J. *Dan. Tidsskr. Farm.* **1972**, *46*, 97.
49. Sanner, M. F. J. *Mol. Graphics Modell.* **1999**, *17*, 57.